Inorg. Chem. **2006**, *45*, 3648–3656

Borohydride, Azide, and Chloride Anions As Terminal Ligands on Fe/Mo/S Clusters. Synthesis, Structure and Characterization of $[(Cl_4\text{-cat})(PPr_3)\ MoFe_3S_4(X)_2]_2(Bu_4N)_4$ and $[(Cl_4\text{-cat})(PPr_3)MoFe_3S_4(PPr_3)(X)]_2(Bu_4N)_2$ ($X = N_3^-$, BH_4^-, Cl^-) Double-Fused Cubanes. NMR Reactivity Studies of $[(Cl_4\text{-cat})(PPr_3)\ MoFe_3S_4(BH_4)_2]_2(Bu_4N)_4$

Markos Koutmos, Irene P. Georgakaki, and Dimitri Coucouvanis*

Department of Chemistry, University of Michigan, Ann Arbor, Michigan 48109

Received December 19, 2005

Our explorations of the reactivity of Fe/Mo/S clusters of some relevance to the FeMoco nitrogenase have led to new double-fused cubane clusters with the $Mo_2Fe_6S_8$ core as derivatives of the known $(Cl_4\text{-cat})_2Mo_2Fe_6S_8(PPr_3)_6$ (**I**) fused double cubane. The new clusters have been obtained by substitution reactions of the PPr_3 ligands with Cl^-, BH_4^-, and N_3^-. By careful control of the conditions of these reactions, the clusters $[(Cl_4\text{-cat})(PPr_3)MoFe_3S_4(BH_4)_2]_2(Bu_4N)_4$ (**II**), $[(Cl_4\text{-cat})(PPr_3)MoFe_3S_4(PPr_3)(BH_4)]_2(Bu_4N)_2$ (**III**), $[(Cl_4\text{-cat})(PPr_3)MoFe_3S_4(N_3)_2]_2(Bu_4N)_4$ (**IV**), $[(Cl_4\text{-cat})(PPr_3)MoFe_3S_4(PPr_3)(N_3)]_2(Bu_4N)_2$ (**V**), and $[(Cl_4\text{-cat})(PPr_3)MoFe_3S_4Cl_2]_2(Et_4N)_4$ (**VI**) have been obtained and structurally characterized. A study of their electrochemistry shows that the reduction potentials for the derivatives of **I** are shifted to more positive values than those of **I**, suggesting a stabilization of the reduced clusters by the anionic ligands BH_4^- and N_3^-. Using ^1H NMR spectroscopy, we have explored the lability of the BH_4^- ligand in **II** in coordinating solvents and its hydridic character, which is apparent in its reactivity toward proton sources such as MeOH or PhOH.

Introduction

Single-crystal X-ray structure determinations of the MoFe protein component of nitrogenase from various sources[1,2] have determined the structure of the unique octanuclear $MoFe_7S_9$ catalytic center at various levels of resolution. This center consists of two cuboidal subunits, $MoFe_3S_3$ and Fe_4S_3, bridged by three μ_2-S^{2-} ligands. The most recent structure determination of the *Azotobacter vinelandii* MoFe protein at 1.16 Å[3] resolution revealed a previously undetected light atom whose identity, being uncertain at present (C, N, or O), has stimulated intense research, as evident by recent theoretical[4] and spectroscopic studies.[5] The encapsulated μ_6-X atom in the center of the Fe_6 unit (Figure 1) is shared

* To whom correspondence should be addressed. E-mail: dcouc@umich.edu.

(1) (a) Kim, J.; Rees, D. C. *Science*, **1992**, *257*, 1677. (b) Howard, J. B.; Rees, D. C. *Chem. Rev.* **1996**, *96*, 2965. (c) Georgiadis, M. M.; Komiya, H.; Woo, D.; Kornuc, J. J.; Rees, D. C. *Science* **1992**, *257*, 1653. (d) Kim, J.; Rees, D. C. *Nature* **1992**, *360*, 553. (e) Chan, M. K.; Kim, J.; Rees, D. C. *Science* **1993**, *260*, 792. (f) Kim, J.; Woo, D.; Rees, D. C. *Biochemistry* **1993**, *32*, 7104. (g) Schindelin, N.; Kisker, C.; Schlessman, J. L.; Howard, J. B.; Rees, D. C. *Nature* **1997**, *387*, 370. (h) Strop, P.; Takahara, P. M.; Chiu, H.-J.; Angove, H. C.; Burgess, B. K.; Rees, D. C. *Biochemistry* **2001**, 40, 651.

(2) (a) Bolin, J. T.; Ronco, A. E.; Morgan, T. V.; Mortenson, L. E.; Xuong, N. *Proc. Natl. Acad. Sci. U.S.A.* **1993**, *90*, 1078. (b) Mayer, S. M.; Lawson, D. M.; Gormal, C. A.; Roe, S. M.; Smith, B. E. *J. Mol. Biol.* **1999**, *292*, 871.

(3) Einsle, O.; Tezcan, A. F.; Andrade, S. L. A.; Schmid, B.; Yoshida, M.; Howard, J. B.; Rees, D. C. *Science* **2002**, *297*, 1696−1700.

(4) (a) Hinneman, B.; Nørskov, J. K. *J. Am. Chem. Soc.* **2003**, *125*, 1466. (b) Dance, I. *Chem. Commun.* **2003**, 324−325. (c) Lovell, T.; Liu, T.; Case, D. A.; Noodleman, L. *J. Am. Chem. Soc.* **2003**, *125*, 8377−8383. (d) Schimpl, J.; Petrill, H. M.; Blochl, P. E. *J. Am. Chem. Soc.* **2003**, *125*, 15772. (e) Dance, I. *J. Am. Chem. Soc.* **2004,** *126*, 11852−11863. (f) Hinnemann, B.; Norskov, J. K. *J. Am. Chem. Soc.* **2004**, *126*, 3920−3927

(5) (a) Lee, H.-I.; Benton, P. M. C.; Laryukhin, M.; Igarashi, R. Y.; Dean, D. R.; Seefeldt, L. C.; Hoffman, B. M. *J. Am. Chem. Soc.* **2003**, *125*, 5604. (b) Barney, B. M.; Igarashi, R. Y.; Dos Santos, P. C.; Dean, D. R.; Seefeldt, L. C. *J. Biol. Chem.* **2004**, *279*, 53621−53624. (c) Lee, H. I.; Igarashi, R. Y.; Laryukhin, M.; Doan, P. E.; Dos Santos, P. C.; Dean, D. R.; Seefeldt, L. C.; Hoffman, B. M. *J. Am. Chem. Soc.* **2004,** *126*, 9563−9569. (d) Vrajmasu, V.; Munck, E.; Bominaar, E. L. *Inorg. Chem.* **2003**, *42*, 5974−5988.

10.1021/ic052156b CCC: $33.50
Published on Web 03/30/2006

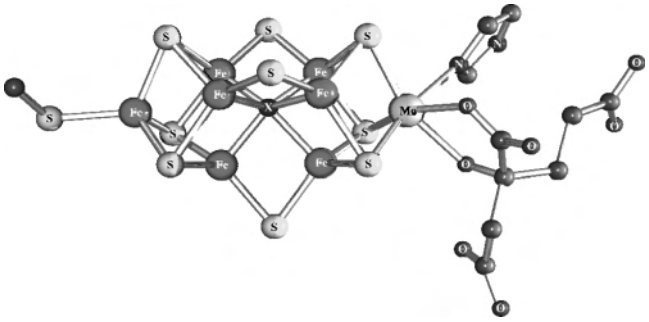

Figure 1. Structure of the FeMoS center of Nitrogenase.

by four-coordinate trigonal-pyramidal Fe atoms. Previously these Fe atoms in the Fe_6 unit were thought to be three-coordinate coordinatively unsaturated sites.

The synthesis and structures of a multitude of high nuclearity Mo/Fe/S structures notwithstanding,[6] exact synthetic analogues for the nitrogenase FeMo cofactor are still not available. Predominant among the plethora of the known Mo/Fe/S clusters are those that contain as a common structural feature one, two, or three $MoFe_3S_4$ "cubane"[7,8,9] and $MoFe_3S_3$[10] cuboidal units. These clusters have contributed significantly to fundamentally important chemistry. The mechanism of dinitrogen activation and reduction by the FeMoS cofactor in nitrogenase has been the subject of numerous calculations and proposals. The variety of theoretical models available underscores the fact that the mechanism of N_2 fixation is still an unresolved problem. The nitrogenases display hydrogenase activity, reducing H^+ to H_2; a process that acts as an inhibitor to NH_3 formation.[11] A proposed N_2-fixation mechanism that involves the possible formation of FeMoco−hydrogen or hydride intermediates has been described recently.[12] In an attempt to explore the possible existence of these proposed metallo−hydrido or hydrogen atom intermediate clusters, we investigated the reactions of the $(Cl_4\text{-cat})_2Mo_2Fe_6S_8(PR_3)_6$ **I** clusters with a hydride source such as the BH_4^- anion. Preliminary findings of this study have been communicated earlier,[13] where the first example of a $MoFe_3S_4$ cluster containing BH_4^- was presented. The synthetic utility of **I** has been well documented. In attempts to further explore the reactivity of **I**, we reacted **I** with a variety of ligands including known substrates of the nitrogenase enzyme such as N_3^-, N_2H_4, and derivatives of it.[11,14] The different reactivity properties of the ligands bound to the Mo and Fe sites have allowed the development of an extensive and site-specific cluster substitution chemistry. We took advantage of these properties to synthesize novel compounds where substitution of the P^nPr_3 phosphines by different ligands involves only those bound to Fe atoms of cluster **I**.

In this paper we provide detailed documentation on the synthesis, molecular structures, and spectroscopic properties of this first example of a $MoFe_3S_4$ cluster that contains BH_4^- ligands, as well examples of a $MoFe_3S_4$ cluster with azides bound to the Fe atoms. Moreover, we were able also to control the substitution of the phosphines bound to Fe atoms, thus allowing us to isolate unique clusters where both phosphines and azides or borohydrides complete the coordination environment of these Fe atoms.

Experimental Section

General. All experiments and reactions were carried out under a dinitrogen atmosphere using standard Schlenk line techniques or in an inert atmosphere glovebox. All solvents were distilled under dinitrogen and degassed using nitrogen. Acetonitrile was predried over oven-dried molecular sieves and distilled over CaH_2. Ethyl ether, THF, and toluene were predried over Na ribbon and further purified by the sodium-benzoketyl method. Tetrachlorocatechol (Cl_4-catH_2) (Lancaster) was dissolved in ethyl ether, and the concentrated solution was treated with activated charcoal (Aldrich). After a few hours, the mixture was filtered by gravity filtration, and the process repeated until the ether solution contained no dark brown color. Once the color of the diethyl ether solution became lighter, the solvent was removed by nitrogen purging, and the residue was dried under vacuum. Anhydrous Et_4NCl, Bu_4NBH_4, and Bu_4NN_3 were purchased from Fluka or Aldrich and used without further purification. Deuterated solvents, as well as methanol-d_4, were purchased from Cambridge Isotope Laboratories. Boric acid-d_3 and phenol-d_6 were purchased from Aldrich. $(Cl_4\text{-cat})_2Mo_2Fe_6S_8(PPr_3)_6$ was synthesized according to the published method.[15]

FT-IR spectra were collected on a Nicolet DX V. 4.56 FT-IR spectrometer in KBr pellets, and the spectra were corrected for background. ^{1}H NMR spectra were recorded on a Unity+ 300 MHz superconducting NMR instrument operating at 299.9 MHz. ^{11}B NMR spectra were recorded on an Innova 500 MHz superconducting NMR instrument operating at 160.38 MHz (Et_2O/BF_3 was used as external standard and referenced to 0 ppm). Elemental analyses were performed by the Microanalytical Laboratory at the University of Michigan. The data were corrected using acetanilide as a standard. Electronic spectra were recorded on a Varian CARY 1E UV−Vis spectrometer. The magnetic susceptibility measurements were carried out on a MPMS SQUID magnetometer, and the data were corrected for diamagnetic contributions. All the cyclic voltammetry experiments were carried out using an EG&G Princeton potensiostat/galvanostat Model 263A and an Ag/AgCl reference electrode with 0.1 M Bu_4NPF_6 as the electrolyte. Ferrocene

(6) Malinak, S. M.; Coucouvanis, D. *Prog. Inorg. Chem*. **2001**, *49*, 599 and references therein.
(7) Lee, S. C.; Holm, R. H. *Chem. Rev*. **2004**, *104*, 1135 and references therein.
(8) (a) Wolff, T. E.; Power, P. P.; Frankel, R. B.; Holm. R. H. *J. Am. Chem. Soc.* **1980**, *102*, 4694. (b) Demadis, K. D.; Campana, C. F.; Coucouvanis, D. *J. Am. Chem. Soc*. **1995**, *117*, 7832. (c) Zhang, Y. G.; Holm, R. H. *J. Am. Chem. Soc.* **2003**, *125*, 3910−3920.
(9) Koutmos, M.; Coucouvanis, D. *Angew. Chem., Int. Ed.* **2004**, *43*, 5023−5025.
(10) (a) Coucouvanis, D.; Han, J.; Moon, N. *J. Am. Chem. Soc*. **2002**, *124*, 216. (b) Tyson, M. A.; Coucouvanis, D. *Inorg. Chem*. **1997**, *36*, 3808. (c) Han, J.; Beck, K.; Ockwig, N.; Coucouvanis, D. *J. Am. Chem. Soc.* **1999**, *121*, 10448.
(11) Burgess, B. K.; Lowe, D. J. *Chem. Rev.* **1996,** 96, 2983−3011 and references therein.
(12) Huniar, U.; Ahlrichs, R.; Coucouvanis, D. *J. Am. Chem. Soc.* **2004**, *126*, 2588.
(13) Koutmos, M.; Coucouvanis, D. *Inorg. Chem.* **2004**, *43*, 6508−6510.
(14) (a)Burgess, B. K. In *Molybdenum Enzymes*; Spiro, T. G., Ed.; Wiley-Interscience: New York, 1985; p 161. (b) Burgess, B. K. In *Molybdenum Enzymes, Cofactors, and Model Systems*; Stiefel, E. I., Coucouvanis, D., Newton, W. E., Eds.; American Chemical Society: Washington, DC, 1993; p 144.
(15) Han, J.; Koutmos, M.; Ahmad, S. A.; Coucouvanis, D. *Inorg. Chem.* **2001**, *40*, 5985.

peak potentials were found at 406 and 486 mV (446mV). The redox potentials were reported versus SCE: (rev) reversible, (qr) quasireversible, (irr) irreversible.

The compounds of primary interest are designated as follows:

$$(Cl_4\text{-cat})_2Mo_2Fe_6S_8(PR_3)_6 \quad (I)$$

$$(Cl_4\text{-cat})_2Mo_2Fe_6S_8(P^nPr_3)_6 \quad (Ia)$$

$$(Cl_4\text{-cat})_2Mo_2Fe_6S_8(PEt_3)_6 \quad (Ib)$$

$$(Cl_4\text{-cat})_2Mo_2Fe_6S_8(P^nBu_3)_6 \quad (Ic)$$

$$[(Cl_4\text{-cat})(P^nPr_3)MoFe_3S_4(BH_4)_2]_2(Bu_4N)_4 \quad (II)$$

$$[(Cl_4\text{-cat})(P^nPr_3)MoFe_3S_4(P^nPr_3)(BH_4)]_2(Bu_4N)_2 \quad (III)$$

$$[(Cl_4\text{-cat})(P^nPr_3)MoFe_3S_4(N_3)_2]_2(Bu_4N)_4 \quad (IV)$$

$$[(Cl_4\text{-cat})(P^nPr_3)MoFe_3S_4(P^nPr_3)(N_3)]_2(Bu_4N)_2 \quad (V)$$

$$[(Cl_4\text{-cat})(P^nPr_3)MoFe_3S_4Cl_2]_2(Et_4N)_4 \quad (VI)$$

$[(Cl_4\text{-cat})(P^nPr_3)MoFe_3S_4(BH_4)_2]_2(Bu_4N)_4$ (II). $(Cl_4\text{-cat})_2Mo_2Fe_6S_8(PPr_3)_6$ (**I**) (0.5 g, 0.22 mmol) was dissolved in 20 mL of tetrahydrofuran (THF), followed by the addition of 0.255 g (0.99 mmol) of $Bu_4N(BH_4)$ in 5 mL of THF dropwise under vigorous stirring. The reaction mixture was stirred overnight and subsequently filtered. Hexanes were allowed to diffuse slowly into the resulting THF filtrate to yield a crystalline product that was washed with copious amounts of ether; 450 mg of product was obtained after the thorough washings (78% yield). Anal. Calcd for **II**, $C_{94}H_{202}B_4Cl_8Fe_6Mo_2N_4O_4P_2S_8$: C, 43.01; H, 7.76; N, 2.13. Found: C, 43.12; H, 7.67; N, 2.06. IR (KBr pellet, cm^{-1}): B−H 2363(m), 2291(m), 2224(m), 2085(m); Cl_4-cat 1439(vs). Magnetic susceptibility (solid): μ_{eff} (2 K) 5.583 μB, μ_{eff} (5 K) 6.78 μB, μ_{eff} (300K) 7.315 μB. EPR (solid): silent. Cyclic voltammetry (THF, mV): −689 (qr).

$[(Cl_4\text{-cat})(PPr_3)MoFe_3S_4(PPr_3)(BH_4)]_2(Bu_4N)_2$ (III). To a stirred solution of 0.3 g (0.13 mmol) of $(Cl_4\text{-cat})_2Mo_2Fe_6S_8(PPr_3)_6$ (**I**) in 100 mL of THF, 67 mg (0.26 mmol) of $Bu_4N(BH_4)$ in 50 mL of THF was added dropwise over a period of 15 min with rigorous stirring. The reaction mixture ws stirred for 3 h, followed by filtration. The volume of the THF filtrate was reduced to 50 mL under a N_2 stream, and it was subsequently layered with 150 mL of ether; 180 mg (58% yield) of a microcrystalline black product was obtained after filtration and thorough washing with copious amounts of toluene and ether. Anal Calcd for **III** $C_{80}H_{164}B_2Cl_8Fe_6Mo_2N_2O_4P_2S_8$: C, 39.53; H, 6.80; N, 1.15. Found: C, 39.86; H, 6.98; N, 1.19. EPR (solid): silent.

$[(Cl_4\text{-cat})(PPr_3)MoFe_3S_4(N_3)_2]_2(Bu_4N)_4$ (IV). $(Cl_4\text{-cat})_2Mo_2Fe_6S_8(PPr_3)_6$ (**I**) (0.6 g, 0.27 mmol) was dissolved in 20 mL of THF, followed by the addition of 0.341 g (1.2 mmol) of Bu_4NN_3 in 15 mL of THF dropwise with vigorous stirring. The reaction mixture was stirred overnight and subsequently filtered. Hexanes were allowed to diffuse slowly into the resulting THF filtrate to yield a crystalline product that as washed with copious amounts of ether (until the washings were clear); 550 mg of product was obtained after the thorough washings (74% yield). Anal. Calcd for **IV** $C_{94}H_{186}Cl_8Fe_6Mo_2N_{16}O_4P_2S_8$: C, 41.30; H, 6.86; N, 8.23. Found: C, 41.52; H, 6.93; N, 8.18. Magnetic susceptibility (solid): μ_{eff} (2 K) 5.93 μ_B, μ_{eff} (5 K) μ_B 7.17 μ_B, μ_{eff} (300K) 7.13 μ_B. EPR (solid): silent.

$[(Cl_4\text{-cat})(PPr_3)MoFe_3S_4(PPr_3)(N_3)]_2(Bu_4N)_2$ (V). To a stirred solution of 0.3 g (0.13 mmol) of $(Cl_4\text{-cat})_2Mo_2Fe_6S_8(PPr_3)_6$ (**I**) in 100 mL of THF, 74 mg (0.26 mmol) of $Bu_4N(N_3)$ in 50 mL of THF was added dropwise over a period of 15 min with rigorous stirring. The reaction mixture was stirred for 3 h, followed by filtration. The volume of the THF filtrate ws reduced to 50 mL under a N_2 stream, and it was subsequently layered with 150 mL of ether; 180 mg (58% yield) of a microcrystalline black product was obtained after filtration and thorough washing with copious amounts of toluene and ether. Anal. Calcd for **V** $C_{80}H_{156}Cl_8Fe_6Mo_2N_8O_4P_2S_8$: C, 38.66; H, 6.33; N, 4.51. Found: C, 38.93; H, 6.47; N, 4.57. EPR (solid): silent.

$[(Cl_4\text{-cat})(PPr_3)MoFe_3S_4Cl_2]_2(Et_4N)_4$ (VI). One gram (0.45 mmol) of $(Cl_4\text{-cat})_2Mo_2Fe_6S_8(PPr_3)_6$ (I) was dissolved in 50 mL of THF, followed by the addition of 0.300 g (1.81 mmol) of Et_4NCl in 25 mL of acetonitrile dropwise with vigorous stirring. The reaction mixture was stirred overnight and subsequently filtered. A fine black powder (0.45 g) was obtained after washing thoroughly with THF and ether, and in addition, 0.35 g of product was isolated after the acetonitrile/THF filtrate is taken to dryness under a N_2 stream and the resulting black material was washed with copious amounts of THF and ether. Both black solids have been identified as the same desired product (79% yield). Anal. Calcd for $C_{62}H_{122}C_{l12}Fe_6Mo_2N_4O_4P_2S_8$: C, 32.97; H, 5.44; N, 2.48. Found: C, 33.59; H, 6.01; N, 2.26. IR (KBr pellet, cm^{-1}): Cl_4-cat 1439(vs). EPR (solid): silent.

X-ray Crystallography. Black block-shaped crystals of $[(Cl_4\text{-cat})(PPr_3)MoFe_3S_4(BH_4)_2]_2$ $(Bu_4N)_4$ **(II)** and $[(Cl_4\text{-cat})(PPr_3)MoFe_3S_4(PPr_3)(BH_4)]_2(Bu_4N)_2$ **(III)** were obtained from the slow diffusion of hexanes into a THF solution of the corresponding compounds in room temperature. Black block-shaped crystals of $[(Cl_4\text{-cat})(PPr_3)MoFe_3S_4(N_3)_2]_2(Bu_4N)_4$ **(IV)** and $[(Cl_4\text{-cat})(PPr_3)MoFe_3S_4(PPr_3)(N_3)]_2(Bu_4N)_2$ **(V)** were also acquired: the former from the slow diffusion of hexanes into a toluene solution of **IV** and the latter from the slow diffusion of hexanes to a 4:1 THF/toluene solution of **V**. Black plate-shaped crystals of $[(Cl_4\text{-cat})(PPr_3)MoFe_3S_4Cl_2]_2(Et_4N)_4$ **(VI)** were obtained from the slow diffusion of ether into an acetonitrile solution, and they were isolated by filtration. All diffraction data were collected at the University of Michigan X-ray facility at 150(2) K (except for **VI** which was collected at 158(2) K) using a Bruker SMART CCD-based X-ray diffractometer equipped with an LT-2 low-temperature device and normal focus Mo-target X-ray tube ($\lambda = 0.71073$ Å). The crystal data and structural parameters are shown in Tables 1 and 2. The positions of heavy atoms were found by direct methods in E-maps using the software solution program in SHELXTL, version 6.1.[16] Subsequent cycles of least-squares refinement followed by difference Fourier synthesis produced the positions of the remaining nonhydrogen atoms; they were refined anisotropically (except for a highly distorted Bu_4N^+, a toluene solvent molecule, and a propyl-chain of the PPr_3 phosphine in compound **IV** which were refined isotropically). Positions of the hydrogen atoms of the borohydride ligands in compound **II** were found and located from the final difference Fourier map. These hydrogen atoms, which are essential in defining the structure, were included and refined isotropically. The remaining hydrogen atoms for **II**, as well all hydrogen atoms for **III**, **IV**, **V**, and **VI**, were placed in ideal positions and refined as riding atoms with individual isotropic thermal displacement parameters. Compounds **II**, **IV**, and **VI** crystallized in the space group $P2_1/c$, whereas **III** and **V** crystallized in the space group $P2_1/n$; this was confirmed by the program XPREP of the SHELXTL package.[16]

(16) *SHELXTL*, version 6.10; Siemens Industrial Automation, Inc.: Madison, WI, 2000.

Table 1. Crystal Data and Structure Refinements for $[(Cl_4\text{-cat})(PPr_3)MoFe_3S_4(BH_4)_2]_2(Bu_4N)_4$, **II**, $[(Cl_4\text{-cat})(PPr_3)MoFe_3S_4(N_3)_2]_2(Bu_4N)_4$, **IV**, and $[(Cl_4\text{-cat})(PPr_3)MoFe_3S_4Cl_2]_2(Et_4N)_4$, **VI**

	II	**IV**·tolune	**VI**
empirical formula	$C_{94}H_{202}B_4Cl_8Fe_6Mo_2N_4O_4P_2S_8$	$C_{54}H_{107}Cl_4Fe_3MoN_8O_2PS_4$	$C_{62}H_{122}Cl_{12}Fe_6Mo_2N_4P_2S_4$
fw	2624.84	1464.98	2258.44
cryst syst	monoclinic	monoclinic	monoclinic
space group	$P2_1/c$	$P2_1/c$	$P2_1/c$
a (Å)	17.142(2)	18.688(2)	18.789(9)
b (Å)	22.604(3)	27.301(3)	18.670(9)
c (Å)	17.295(2)	15.226(2)	13.060(6)
α (deg)	90.00	90.00	90.00
β (deg)	110.387(2)	111.696(2)	91.088(8)
γ (deg)	90.00	90.00	90.00
V (Å^3)	6282.0(12)	7218.3(15)	4581(4)
Z, calcd density (mg/mm^3)	2, 1.388	4, 1.348	2, 1.637
temp (K)	150(2)	150(2)	158(2)
abs coeff (mm^{-1})	1.388	1.088	1.797
F(000)	2760	3080	2312
cryst size (mm)	0.40 × 0.36 × 0.34	0.38 × 0.22 × 0.16	0.22 × 0.18 × 0.04
θ range (deg)	2.88−28.44	2.66−22.06	1.90−23.31
limiting indices	$-22 < h < 22$	$-19 < h < 19$	$-20 < h < 20$
	$-30 < k < 29$	$-28 < k < 28$	$-20 < k < 20$
	$-23 < l < 23$	$-16 < l < 16$	$-14 < l < 14$
R(int)	0.0401	0.1023	0.0887
reflns collected	83965	40644	29527
data/restraints/params	15651/0/638	8860/0/614	6609/0/446
final R indices [$I > 2\sigma(I)$] R1, wR2	0.0330, 0.0820	0.0889, 0.2293	0.0433, 0.0937
R indices (all data) R1, wR2	0.0483, 0.0892	0.1531, 0.2914	0.0872, 0.1094
GOF on F^2	1.026	1.093	1.044

Table 2. Crystal Data and Structure Refinements for $[(Cl_4\text{-cat})(PPr_3)MoFe_3S_4(PPr_3)(BH_4)]_2(Bu_4N)_2$, **III**, and $[[(Cl_4\text{-cat})(PPr_3)MoFe_3S_4(PPr_3)(N_3)]_2(Bu_4N)_2$, **V**

	III·hexane	**V**·1/2toluene
empirical formula	$C_{46}H_{96}BCl_4Fe_3MoNO_2P_2S_4$	$C_{47}H_{86}Cl_4Fe_3MoN_4O_2P_2S_4$
fw	1301.52	1334.67
cryst syst	monoclinic	monoclinic
space group	$P2_1/n$	$P2_1/n$
a (Å)	13.525(3)	13.946(2)
b (Å)	17.705(5)	17.381(2)
c (Å)	25.930(7)	25.858(3)
α (deg)	90.00	90.00
β (deg)	96.793(4)	95.866(2)
γ (deg)	90.00	90.00
V (Å^3)	6166(3)	6235.2(13)
Z, calcd density (mg/mm^3)	4, 1.402	4, 1.422
temp (K)	150(2)	150(2)
abs coeff (mm^{-1})	1.285	1.275
F(000)	2728	2776
cryst size (mm)	0.48 × 0.32 × 0.32	0.48 × 0.32 × 0.20
θ range (deg)	2.82−26.50	2.77−26.43
limiting indices	$-16 < h < 16$	$-17 < h < 17$
	$-22 < k < 22$	$-21 < k < 21$
	$-32 < l < 32$	$-32 < l < 32$
R(int)	0.0648	0.0564
reflns collected	55189	51727
data/restraints/params	12632/0/533	12770/0/615
final R indices [$I > 2\sigma(I)$] R1, wR2	0.0811, 0.2119	0.0417, 0.0938
R indices (all data) R1, wR2	0.1409, 0.2569	0.0755, 0.1073
GOF on F^2	1.072	1.025

Results and Discussion

Synthesis. The reaction of $(Cl_4\text{-cat})_2Mo_2Fe_6S_8(PPr_3)_6$ (**I**) with 4 equiv of a ligand such as BH_4^-, N_3^-, or Cl^- in THF proceeds with the substitution of the 4 phosphines bound to the Fe atoms (eq 1). When **I** is treated with 4 equiv of $Bu_4N(N_3)$ in toluene rather than in THF solution, two different products could be isolated. The precipitate of the reaction after recrystallization from THF/ether yields the $[(Cl_4\text{-cat})(PPr_3)MoFe_3S_4(PPr_3)(N_3)]_2(Bu_4N)_2$ **(V)** cluster, whereas cluster $[(Cl_4\text{-cat})(PPr_3)MoFe_3S_4(N_3)_2]_2(Bu_4N)_4$ **(IV)** can be isolated from the filtrate of the reaction mixture, following diffusion of diethyl ether. The same behavior was observed also for the reaction of **I** with 4 equiv of Bu_4NBH_4 in toluene. The problem in both cases is the isolation of analytically pure compounds. We were able to isolate pure material (**III** and **V**) after the reaction of **I** with 2 equiv of Bu_4NBH_4 or 2 equiv of $Bu_4N(N_3)$, respectively, in THF in high dilution and after recrystallization and careful washing (eq 2). In this way we were successful in producing site differentiated compounds where both ligand phosphines and the X^- anions are bound to the Fe atoms.

$$(Cl_4\text{-cat})_2(PPr_3)_2Mo_2Fe_6S_8(PPr_3)_4 + 4X^- \rightarrow [(Cl_4\text{-cat})_2(PPr_3)_2Mo_2Fe_6S_8X_4]^{4-} + 4PPr_3 \quad (1)$$

$$(Cl_4\text{-cat})_2(PPr_3)_2Mo_2Fe_6S_8(PPr_3)_4 + 2X^- \rightarrow [(Cl_4\text{-cat})_2(PPr_3)_2Mo_2Fe_6S_8(PPr_3)_2X_2]^{2-} + 2PPr_3 \quad (2)$$

The substitution of phoshines by Cl^- and N_3^- ligands in $[(Tp)_2V_2Fe_6S_8(PEt_3)_4]$ and $[(Tp)_2Mo_2Fe_6S_8(PEt_3)_4]$ (Tp = tris(pyrazolyl)hydroborate) already has been documented. In these cases, the Mo site is protected from the nucleophilic attack by the tridentate Tp ligand.[17] In our experiment, there is a phosphine and a bidentate Cl_4-cat bound to the Mo instead of the Tp ligand, so replacement of this phosphine seems possible. However, even in the presence of excess of a nucleophilic ligand no products where the Mo-bound phosphine had been replaced could be observed or isolated. Attempts to synthesize one or three phosphine-substituted clusters by carefully controlling the stoichiometry and the

(17) (a) Zhang, Y.; Holm, R. H. *Inorg. Chem.* **2004**, *43*, 674−682. (b) Hauser, C.; Bill, E.; Holm, R. H. *Inorg. Chem.* **2002,** *41*, 1615−1624.

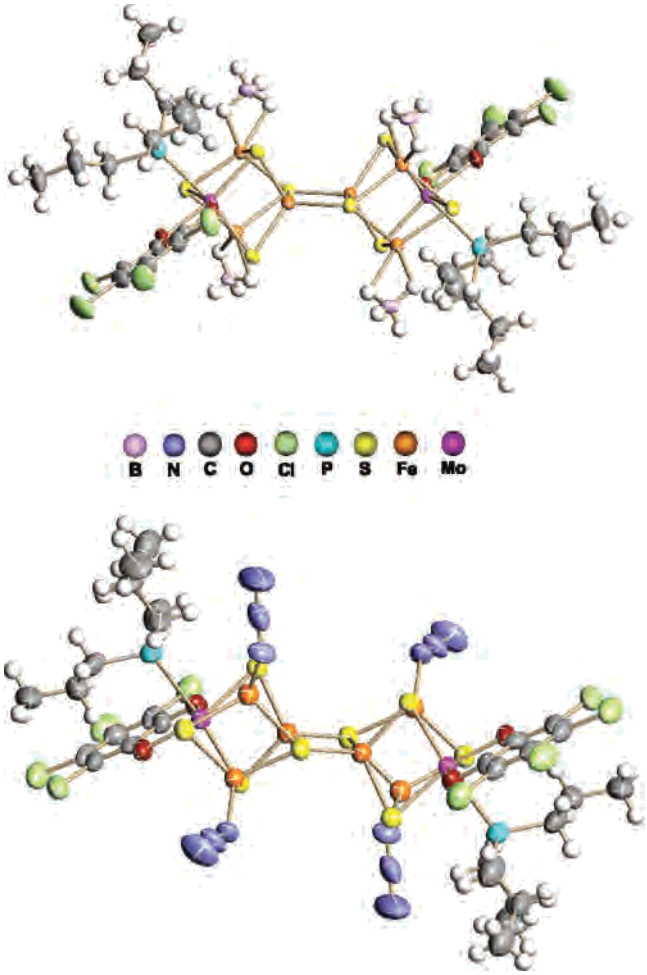

Figure 2. ORTEP diagrams of clusters $[(Cl_4\text{-cat})(PPr_3)MoFe_3S_4(BH_4)_2]_2(Bu_4N)_4$, **II**, and $[(Cl_4\text{-cat})(PPr_3)MoFe_3S_4(N_3)_2]_2(Bu_4N)_4$, **IV**, showing thermal ellipsoids at 50% probability. For clarity the Bu_4N^+ counterions have been omitted.

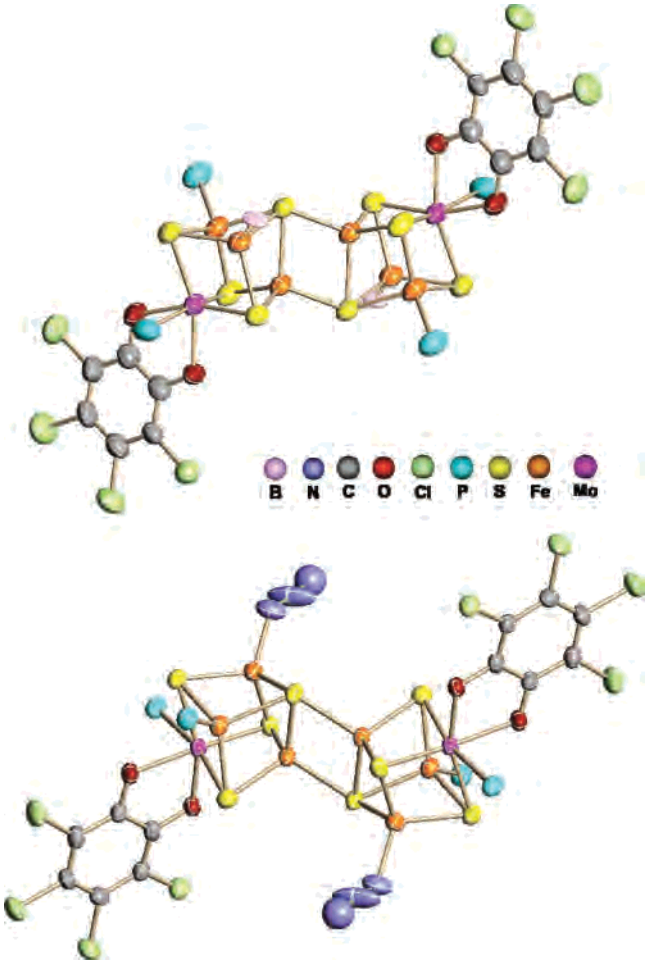

Figure 3. ORTEP diagrams of clusters $[(Cl_4\text{-cat})(PPr_3)MoFe_3S_4(PPr_3)(BH_4)]_2(Bu_4N)_2$, **III**, and $[(Cl_4\text{-cat})(PPr_3)MoFe_3S_4(PPr_3)(N_3)]_2(Bu_4N)_2$, **V**, showing thermal ellipsoids at 50% probability. For clarity the carbon and hydrogen atoms of the propyl groups of the phosphine ligands and the borohydride atoms, as well as the Bu_4N^+ counterions have been omitted.

reaction conditions have been unsuccessful thus far, leading to mixtures of two- and four-substituted phosphine clusters.

Structural Description. All the clusters that are obtained from the reaction of **I** with the ligands BH_4^-, N_3^-, and Cl^- (**II**−**VI**) exhibit the same two edge-sharing $[MoFe_3S_4]$ "cubane" units that define an octanuclear cluster as seen in cluster **I**. The bridge between the two $[MoFe_3S_4]^{2+}$ units in **II**−**VI** defines a $[Fe_2S_2]$ rhomb which has short Fe−Fe distances of 2.6692(6), 2.650(3), 2.630(3), 2.6898(10), and 2.703(2) Å for **II**, **III**, **IV**, **V**, and **VI**, respectively, comparable to those of clusters **Ib** and **Ic** (at 2.659(15) and 2.6512(17) Å, respectively (**Ib**, $(Cl_4\text{-cat})_2Mo_2Fe_6S_8(PEt_3)_6$; **Ic**, $(Cl_4\text{-cat})_2Mo_2Fe_6S_8(P^nBu_3)_6$).[18] The distances in the Fe_2S_2 bridging unit in all clusters are comparable and show only small differences that do not follow any particular trend suggesting that the substitution of the phosphine ligands with anionic ones does not perturb this unit.

The iron atoms can be distinguished in two types. (i) The two atoms (Fe_b) that compose the Fe_2S_2 bridging unit. These are distorted tetrahedral atoms, and they are coordinated only by sulfur atoms, two μ_3-S^{2-} and two μ_4-S^{2-} ligands with average Fe−μ_3-S^{2-} intracubane distances at 2.237(2,3), 2.235(2,4), 2.232(2,4), 2.240(2,8), and 2.244(2,9) Å for **II**, **III**, **IV**, **V**, and **VI**, respectively. The two Fe−μ_4S^{2-} bonds can be distinguished into a short intercubane one and a long intracubane one. Characteristically for the clusters **II**, **III**, **IV**, **V**, and **VI**, the Fe−μ_4S^{2-} intercubane distances are 2.2351(6), 2.253(2), 2.231(4), 2.2690(11), and 2.2312(19) Å, respectively, whereas the Fe − μ_4S^{2-} intracubane distances are 2.3279(6), 2.356(2), 2.333(3), 2.3756(10), and 2.3006(19) Å, respectively. (ii) The remaining four iron atoms, Fe_a, also have a distorted tetrahedral coordination with two μ_4-S^{2-} ligands, one μ_4-S^{2-} ligand, and an anionic ligand such as N^{3-}, Cl^-, a $^nPr_3$ group, in the cases of clusters **IV**, **V**, and **VI**, a 5-coordinate group, as in the case of cluster **II**, and a 4- and 5-coordinate group, in the case of cluster **III** with two μ_4-S^{2-} ligands, one μ_4-S^{2-} ligand, and a bidentate BH_4^- or $^nPr_3$ ligand. The average Fe_a−S distances are 2.305(6,14), 2.283(6,24), 2.285(6,16), 2.273(6,24), and 2.292(6,14) Å, respectively. It is of interest to compare these distances to the corresponding ones of **Ib** and **Ic** at 2.258(6,19) and 2.247(6,12) Å, respectively, since it indicates the influence of the substitution of the phosphine by a better σ-donor, such

(18) Because of the lack of good structural data for compound **Ia**, $[(Cl_4\text{-cat})_2Mo_2Fe_6S_8(PEt_3)_6]$, **Ib**, and $[(Cl_4\text{-cat})_2Mo_2Fe_6S_8(P^nBu_3)_6]$, **Ic**, have been used for the comparison of the two structures

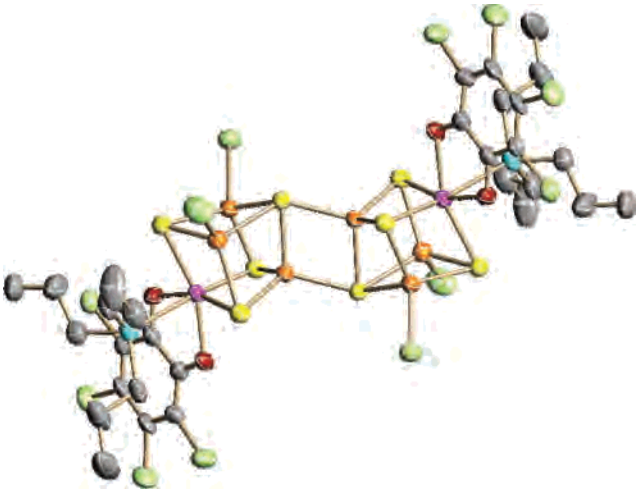

Figure 4. ORTEP diagram of cluster $[(Cl_4\text{-cat})(PPr_3)MoFe_3S_4Cl_2]_2(Et_4N)_2$, **VI**, showing thermal ellipsoids at 50% probability. For clarity the hydrogen atoms of the propyl groups of the phosphine ligands as well as the Et_4N^+ counterions have been omitted.

as the anions mentioned above. Closer examination of the Fe_a coordination environment of $[(Cl_4\text{-cat})(PPr_3)MoFe_3S_4(PPr_3)(BH_4)]_2(Bu_4N)_2$ **III** and $[[(Cl_4\text{-cat})(PPr_3)MoFe_3S_4(PPr_3)(N_3)]_2(Bu_4N)_2$ **V**, where both phosphines and borohydrides or azides are present, shows that the Fe_a atoms that are coordinated by the former (BH_4^-) have an average Fe−S distance of 2.252 and 2.248 Å for **III** and **V**, respectively, whereas for the Fe_a atoms that are coordinated the latter (N_3^-), the corresponding distances are at 2.314 and 2.299 Å for **III** and **V**, respectively. The better electron donors result in the slight elongation and weakening of the Fe−S bonds.

The Mo atoms in all these clusters retain their original distorted MoO_2PS_3 octahedral environment. This environment consists of a $^nPPr_3$ group, three μ_3-S^{2-} ligands, and a bidentate Cl_4cat^{2-} ligand. The average Mo−S distance can be found at 2.365(1) Å (range of Mo−S is 2.351(1)−2.392(1) Å) for **II**, 2.376(2) Å (range of Mo − S is 2.356(2)−2.407(3) Å) for **III**, 2.376(3) Å (range of Mo−S is 2.363(3)−2.401(3) Å) for **IV**, 2.382(1) Å (range of Mo − S is 2.359(1)−2.416-(1) Å) for **V**, and 2.373(2) Å (range of Mo−S is 2.356(2)−2.397(2) Å)for **VI** . All five clusters exhibit a long Mo−S bond (∼0.05 Å), compared to the other two, that corresponds to the one trans to the Mo−P bond. The average Mo−P distances are 2.598(1), 2.600(3), 2.583(4), 2.583(1), and 2.627(2) Å for **II**, **III**, **IV**, **V**, and **VI,** respectively. The differences in the Mo−S and Mo−P bond lengths between all five clusters are insignificant. Furthermore these bond lengths are comparable to the corresponding ones of clusters **Ib** and **Ic.** Thus, it is evident that phosphine substitution of the Fe atoms does not appear to affect the environment around the Mo atom.

The average Mo−Fe distance is 2.719(1) Å (range of 2.703(1)−2.732(1) Å) in **II**, 2.695(3) Å (range of 2.661(3)−2.719(3) Å) in **III**, 2.695(2) Å (range of 2.685(2)−2.703(2) Å) in **IV**, 2.696(1) Å (range of 2.689(1)−2.708(1) Å) in **V**, and 2.723(1) Å (range of 2.708(1)−2.741(2) Å) in **VI,** whereas those in clusters **IIb** and **IIc** are 2.677(5) (range of 2.658(5)−2.695(5) Å) and 2.665(1) Å (range of 2.648(1)−2.681(1) Å), respectively. The average Fe−Fe intracubane distance is 2.735(1) Å (range of 2.704(1)−2.794(1) Å) in **II**, 2.684(3) Å (range of 2.657(3)−2.727(3) Å) in **III**, 2.685(2) Å (range of 2.668(2)−2.696(2) Å) in **IV**, 2.652(1) Å (range of 2.610(1)−2.700(1) Å) in **V**, and 2.684(1) Å (range of 2.648(1)−2.723(2) Å) in **VI**, whereas those in clusters **Ib** and **Ic** are found at 2.634(5) (range of 2.631(5)−2.639(5) Å) and 2.622(1) Å (range of 2.612(1)−2.630(1) Å), respectively. There is a considerable increase in the Fe−Fe bond distances upon substitution of the phosphines bound to the Fe atoms with better electron donors, such as the Cl^-, N^{3-}, and BH_4^- anions, and the increase is more pronounced for $[(Cl_4\text{-cat})(PPr_3)MoFe_3S_4(BH_4)_2]_2(Bu_4N)_4$ **(II)**, about 0.1 Å, compared to clusters **Ib** and **Ic**. This increase in bond distance is also evident from the comparison of the Mo−Mo distances of 7.931(1) Å in **II**, 7.901(3) Å in **III**, 7.881-(2) Å in **IV**, 7.919(2) Å in **V**, and 8.017(1) Å in **VI,** while those of clusters **IIb** and **IIc** are 7.864(2) and 7.849(2) Å, respectively.

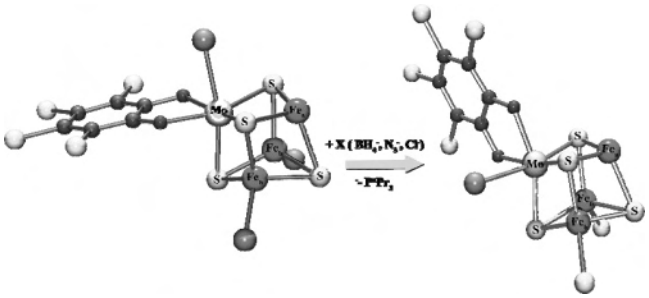

Figure 5. Partial view of clusters **I** and **II**−**VI** demonstrating the difference in arrangement around the Mo atom. Only half of the clusters is depicted in these drawings; the carbon atoms of the phosphines and the counterions have been omitted for clarity.

Closer examination of the Mo coordination environment in clusters **II**−**VI** reveals that the arrangement of the ligands around it is different in these clusters than it is clusters **Ib** and **Ic**. In clusters **Ib** and **Ic**, the Cl_4-catecholate ligands are parallel to the plane defined by the $MoFe_aS_2$ rhombic unit, whereas in clusters **II**−**VI** it is almost perpendicular (Figure 5). This difference indicates that the exchange of the phosphine ligands of the Fe atoms with the borohydride ones is not a simple substitution reaction. It affects the coordination around the Mo atom since bond breaking and formation is required to accommodate the new orientation of the Cl_4-catecholate ligands. The mechanism of this rearrangement is still somewhat unclear.

In clusters **II** and **III**, as already mentioned, we have the substitution of phosphine ligands with borohydride ones. The IR spectra at the B−H stretching region for both compounds are almost identical (only small differences in the relative intensity of the peaks) and indicative of a bidentate binding mode,[19] with a 139 cm^{-1} separation between the μ-B−H (terminal) and μ-B−H (bridging) modes. That is suggestive of a rather weak M−BH_4 interaction. This is confirmed by the X-ray crystal structure of **II** where the average Fe−H_b

(19) (a) Marks, T. J.; Kennelly, W. J.; Kolb, J. R.; Shimp, L. A. *Inorg. Chem.* **1972**, *11*, 2540. (b) Marks, T. J.; Kolb, J. R. *Chem. Rev.* **1977**, *77*, 263.

Table 3. Selected Bond distances (Å)

	Ib, Ic	II	III	IV	V	VI
Fe_b-Fe_b	2.659(15), 2.651(2)	2.6692(6)	2.650(3)	2.630(3)	2.6898(10)	2.703(2)
$Fe_b-\mu_3$-S		2.237(2,3)[a]	2.235(2,4)[a]	2.232(2,4)[a]	2.240(2,8)[a]	2.244(2,9)[a]
$Fe_b-\mu_4-S_{intercubane}$		2.2351(6)	2.253(2)	2.231(4)	2.2690(11)	2.2312(19)
$Fe_b-\mu_4-S_{intracubane}$		2.3279(6)	2.356(2)	2.333(3)	2.3756(10)	2.3006(19)
Fe_a-S	2.258(6,19),[a] 2.247(6,12)[a]	2.305(6,14)[a]	2.283(6,24)[a]	2.285(6,16)[a]	2.273(6,24)[a]	2.292(6,14)[a]
Mo−S		2.365[b]	2.376[b]	2.376[b]	2.382[b]	2.373[b]
Mo−P		2.598(1)	2.600(3)	2.583(4)	2.583(1)	2.627(2)
Mo−Fe	2.634,[c] 2.622 [c]	2.719[c]	2.695	2.695[c]	2.696[c]	2.723[c]
Fe_a-N				1.955(2,9)	1.942	
Fe_a-B		2.304(2,21)[a]	2.302			
Fe_a-Cl						2.248(2,1)[a]

[a] The first number in parentheses indicates the number of distances that are averaged, while the second number indicates the standard deviation. [b] Range of Mo−S distances: 2.351(1)−2.392(1), 2.356(2)−2.407(3), 2.363(3)−2.401(3), 2.359(1)−2.416(1), and 2.356(2)−2.397(2) Å for **II**, **III**, **IV**, **V**, and **VI**, respectively. [c] Range of Mo−Fe distances: 2.658(5)−2.695(5), 2.648(1)−2.681(1), 2.703(1)−2.732(1), 2.661(3)−2.719(3), 2.685(2)−2.703(2), 2.689(1)−2.708(1), and 2.708(1)−2.741(2) for **Ib**, **Ic**, **II**, **III**, **IV**, **V**, and **VI**, respectively.

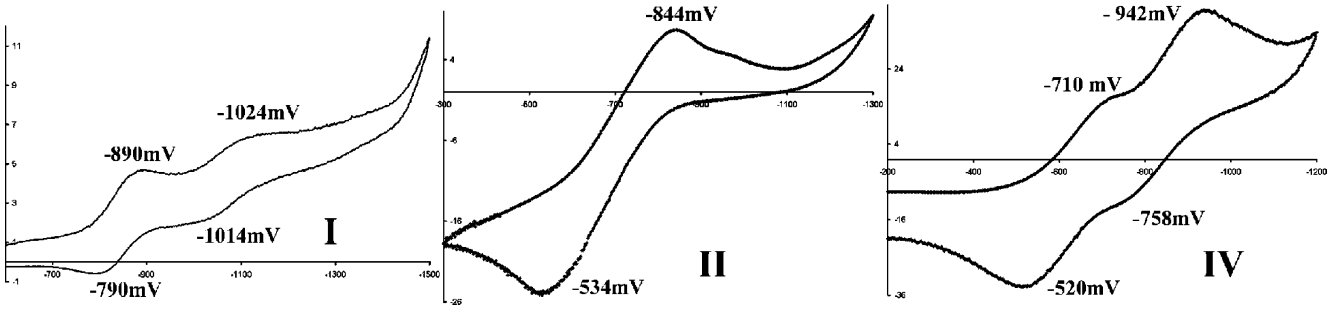

Figure 6. Representative cyclic voltammograms of clusters, $(Cl_4\text{-cat})_2Mo_2Fe_6S_8(PPr_3)_6$, **Ia**, $[(Cl_4\text{-cat})(PPr_3)MoFe_3S_4(BH_4)_2]_2(Bu_4N)_4$, **II**, and $[(Cl_4\text{-cat})(PPr_3)MoFe_3S_4(N_3)_2]_2(Bu_4N)_4$, **IV**. Peak potentials are indicated.

distances are rather long at 1.903 Å (range of 1.821−1.977 Å). The B−H distances and H−B−H angles reveal an almost ideal tetrahedral arrangement around the boron atom. The BH_4^- unit occupies, through two bridging hydrogens, two coordination sites around the iron atoms, but it is thereby forced to a very small average H−Fe−H bite angle of 51.55°. The Fe−B distances are 2.289(3) and 2.319(3) Å for cluster **II** and 2.302(6) Å for cluster **III**. In $[(Cl_4cat)(^nPr_3P)Mo_2Fe_3S_4(BH_4)_2]_2(Bu_4N)_4$ (**II**), the four Fe_a atoms are five-coordinated, whereas in cluster **III**, two Fe_a atoms are five-coordinated (the ones coordinated by the BH_4^- groups) and the other two four-coordinated. This renders cluster **III** a rather unique cluster where the Fe atoms of the cluster are in various different chemical and coordination environments.

The $Fe-N_{azide}$ distances are 1.962(11) and 1.949(12) Å for **IV** and 1.942(4) Å for **V**. The coordinated azide ions in cluster **IV** and **V** are almost linear with two inequivalent N−N distances. This difference is not unusual and reflects the different resonance forms of bound azides. The Fe−N−N angles in **IV** are 138.78 and 132.89°, while in **V**, the angle is 133.99° Both complexes exhibit the same strong asymmetric azide stretch (different relative intensities) at 2056 cm^{-1} in the IR spectra indicating the same chemical environment.

Electrochemistry and Magnetic Properties. The substitution of the phosphine ligands with anionic BH_4^-, N_3^-, or Cl^- ligands affects the reduction potential of the final products; this is evident in their electrochemical behaviors. The cyclic voltammetry of cluster **II** exhibits only a single quasireversible reduction at −689 mV compared to those of cluster **Ia** at −840 and −1069 mV. The electrochemistry hints at the possible formation of a different product after the one-electron reduction. The electrochemical behavior of **IV** is rather different than that of **II** and similar to that of **I**, displaying two reversible reduction waves that are occurring at −611 and −861 mV. Clearly, the azide substitution of the phoshine ligands leads to a decrease in the reduction potentials. On the other hand, cluster **III** shows a quasireversible single reduction at −763 mV (slightly shifted to a more negative value than that of **II**), whereas **V** shows two reductions at −752 and −1006 mV (significantly higher than that of **IV**).

The magnetic susceptibility of **II** was measured over various temperatures, and it shows a maximum effective magnetic moment of 7.57 μ_B at 145 K (Figure 7). The magnetic moment decreases gradually to 7.32 μ_B when the temperature increases from 145 to 300 K. Below 115 K, the magnetic moment decreases gradually, and below 20 K, it decreases steeply to 5.58 at 2 K. The magnetic moment of **IV** shows a steep increase from 5.93 μ_B at 2 K, to 7.55 at 17 K, its maximum value, and subsequently, it decreases gradually to 7.12 at 300 K. On the other hand, cluster **IV** exhibits a steep increase in its effective magnetic moment from 6.97 μ_B at 5 K to 7.21 μ_B at 28 K, remains almost constant until 135 K, and then increases to 7.41 μ_B at 300 K. The magnetic behaviors of all the clusters mentioned

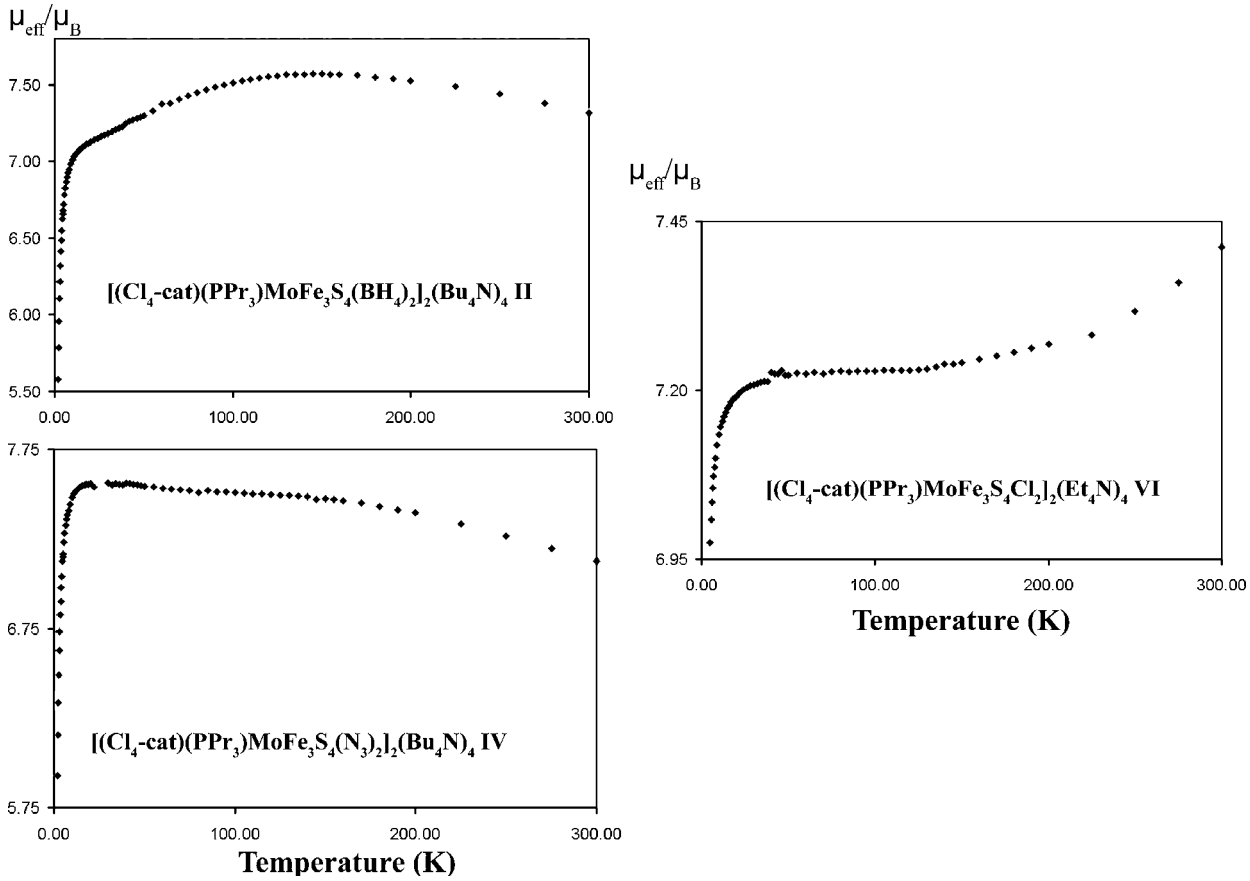

Figure 7. Effective magnetic moments of clusters $[(Cl_4\text{-cat})(PPr_3)MoFe_3S_4(BH_4)_2]_2(Bu_4N)_4$, **II**, $[(Cl_4\text{-cat})(PPr_3)MoFe_3S_4(N_3)_2]_2(Bu_4N)_4$, **IV**, and $[(Cl_4\text{-cat})(PPr_3)MoFe_3S_4Cl_2]_2(Et_4N)_4$, **VI**, plotted versus temperature.

above suggest rather complicated antiferromagnetic coupling. These magnetic behaviors are comparable to those of clusters **Ia**, **Ib**, and **Ic** and, in addition to the silent EPR spectra of clusters **II**−**VI**, indicate that the oxidation states of the metal centers are not affected by the substitution reactions.

NMR Studies. Solution Structure of $[(Cl_4cat)(Pr_3P)Mo_2Fe_3S_4(BH_4)_2]_2(Bu_4N)_4$ (II). NMR studies reveal the BH_4^- ligand lability of **II** in coordinating solvents. The ^{1}H NMR spectrum of compound **II** in the borohydride region in CD_3CN or THF-d_8 shows a quartet centered at −0.25 ppm with an average J_{B-H} of 82.5 Hz. Free BH_4^- of Bu_4NBH_4 in the same solvents gives a quartet at the same chemical shift with $J_{B-H} = 81$ Hz. This similarity of the chemical shift and the coupling constant of BH_4^- anion in **II** with those of the free anion indicates dissociation of BH_4^- in a solution of **II** in coordinating solvents. The absence of any BH_4^- resonance in the ^{1}H NMR spectrum of **II** in toluene-d_8 indicated that the coordinated BH_4^- ligand does not dissociate but hints that the metal-bound BH_4^- cannot be observed in the ^{1}H NMR spectrum of **II** using the same experimental parameters, probably because it is coordinated to a paramagnetic Fe center. ^{11}B NMR experiments were also carried out in acetonitrile and toluene to obtain additional information on the lability of the system. The ^{11}B NMR chemical shifts of **II**, as compared to Bu_4NBH_4, were not conclusive as to if free BH_4^- was present in the acetonitrile solution of **II**, a fact that was only indicated by ^{1}H NMR.

To further investigate the BH_4^- dissociation process, a variable-temperature (VT) ^{1}H NMR experiment was run in CD_3CN in the temperature range of 25−70 °C. From this study it became obvious that the dissociation of BH_4^- increases with temperature, and it is an irreversible process as indicated by the ^{1}H NMR spectrum of the sample when cooled to room temperature after the high-temperature experiment. Attempts to characterize the product of BH_4^- dissociation thus far have been unsuccessful, however it seems likely that BH_4^- is substituted by CD_3CN.

Reactivity of $[(Cl_4cat)(Pr_3P)Mo_2Fe_3S_4(BH_4)_2]_2(Bu_4N)_4$ toward MeOH and Phenol. The reaction of **II** with deuterated MeOD and PhOD carried out in an NMR tube was studied using ^{1}H NMR spectroscopy, the results of which are discussed below. The ^{1}H NMR spectrum of **II** was taken before and after the addition of small amounts of the above reagents. In all cases, the formation of H_2 and HD in the ^{1}H NMR spectrum was shown by the appearance of two peaks, a singlet at ∼4.57 ppm and a triplet centered at ∼4.53 ppm ($J_{H-D} = 42.9$ Hz).[20] It should be mentioned that even before the addition of any deuterated proton source there was a small amount of H_2 formed in a solution of **II** in CD_3CN but not in toluene-d_8. A possible explanation could be the formation of the adduct $CD_3CN{\cdot}BH_3$ and a metal-bound hydride that is unstable and undergoes 1e$^-$ transfer to the metal cluster

(20) (a) Sellmann, D.; Fürsattel, A. *Angew. Chem.* **1999**, *38*, 2023. (b) Zhao, X.; Georgakaki, I. P.; Miller, M. L.; Mejia-Rodriguez, R.; Chiang, C.-Y.; Darensbourg, M. Y. *Inorg. Chem.* **2002**, *41*, 3917.

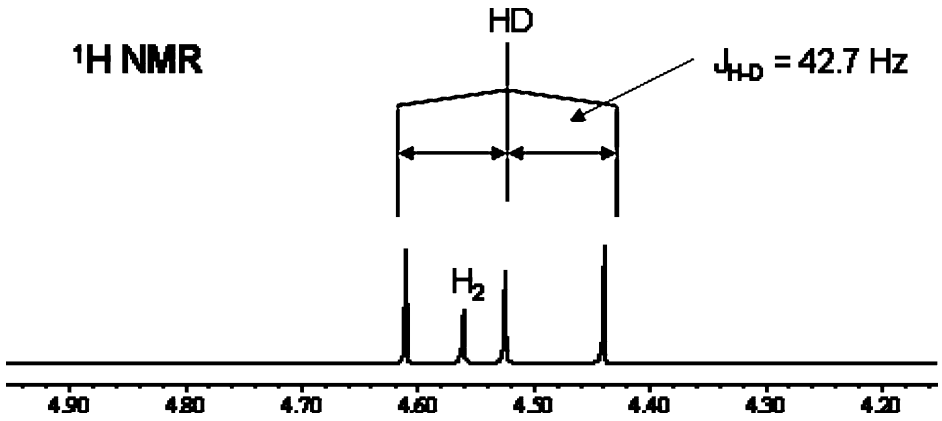

Figure 8. H_2 and HD evolution as evident in the section of the ^{1}H NMR spectra after addition of CH_3OD in a solution of **II** in toluene-d_8.

and releases H_2. Alternatively, H_2 and HD could be formed from BH_4^- in the presence of the acidic CD_3CN given that it is not 100% deuterated. When PhOD was added to CD_3CN solution of **II**, the formation of H_2 was greater than that of HD. When MeOD was added, however, in the same solvent, the formation of H_2 and HD were of about the same amount. The opposite happened when MeOD was added to toluene-d_8 solutions of **II** where HD was more than H_2 in the first 7 h (Figure 8). After the mixture stood overnight, the intensity of the resonance corresponding to H_2 became greater than HD. Since the dissociation of BH_4^- in coordinating solvents has been established, in the cases where CD_3CN was used, the formation of HD and H_2 was attributed to the reactivity of both the free and the metal-bound BH_4^- toward these proton sources (MeOD and PhOD). In toluene-d_8, the formation of HD and H_2 was the result of the metal-bound BH_4^- in **II**. The absence of any resonance in the region of BH_4^- in the ^{1}H NMR spectrum of **II** excludes the presence of free BH_4^- in solution either before or after the addition of the deuterated reagent. The formation of H_2 and HD from **II** in the presence of MeOD or PhOD is in agreement with the reactivity of the hydridic BH_4^- toward a proton source according to the following equation

$$BH_4^- + MeOD \rightarrow\rightarrow HD + BH_3OMe \text{ or } H_2 + BDH_2OMe$$

In CD_3CN solution, initially, after the addition of the proton source, there is more H_2 that HD, while in toluene-d_8 the opposite happens; this is explained by the fact that there is a parallel process of formation of H_2 in CD_3CN (see above). After they stood overnight, the amount H_2 in all solutions is greater that HD; this is consistent with the statistical mixture predicted from the above equation. No NMR evidence was found for coordinated H^-, as a result of BH_3 addition to the Lewis-basic solvent molecules.

Summary

Phosphine/L substitution reactions in $(Cl_4\text{-cat})_2Mo_2Fe_6S_8(PPr_3)_6$ (**I**) yielded a number of new clusters $(Cl_4\text{-cat})_2Mo_2(PPr_3)_2Fe_6S_8(PPr_3)_{4-x}L_x(R_4N)_x$ based on the double-fused cubane $Mo_2Fe_6S_8$ core, where $L = N_3^-$, BH_4^- or Cl^- and $x = 2$ or 4. Compounds **II** and **III** have BH_4^- coordinated to Fe atoms and could provide starting materials for biologically relevant metallo-sulfur-hydrido clusters. Thus far we have been unable to detect the latter in solution. Compounds **IV** and **V** with N_3^- bound to Fe may prove to be reagents for the incorporation of nitrides into the MoFeS clusters given that $Fe-N_3$ has been reported to undergo transformation via photolysis or other chemical means to Fe≡N nitrides.[21] Work in this area is in progress.

Acknowledgment. We thank Dr. Jeff Kampf for X-ray data collection. The authors acknowledge the support of this work by a grant from the National Institutes of Health (GM 33080).

Supporting Information Available: X-ray crystallographic file in CIF format for $[(Cl_4\text{-cat})(PPr_3)MoFe_3S_4(BH_4)_2]_2(Bu_4N)_4$, $[(Cl_4\text{-cat})(PPr_3)MoFe_3S_4(PPr_3)(BH_4)]_2(Bu_4N)_2$, $[(Cl_4\text{-cat})(PPr_3)MoFe_3S_4(N_3)_2]_2(Bu_4N)_4$, $[(Cl_4\text{-cat})(PPr_3)MoFe_3S_4(PPr_3)(N_3)]_2(Bu_4N)_2$, and $[(Cl_4\text{-cat})(PPr_3)MoFe_3S_4Cl_2]_2(Et_4N)_2$. This material is available free of charge via the Internet at http://pubs.acs.org.

IC052156B

(21) Dutta, S. K.; Beckmann, U.; Bill, E.; Weyhermuller, T.; Wieghardt, K. *Inorg. Chem.* **2000**, *39*, 3355−3364.